ChemComm

Accepted Manuscript

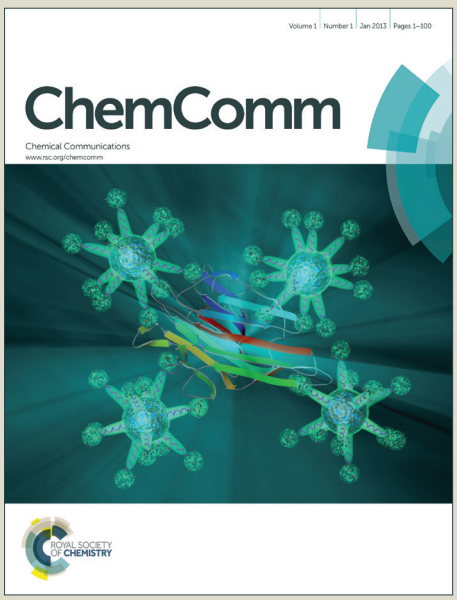

ROYAL SOCIETY OF CHEMISTRY

www.rsc.org/chemcomm

Journal Name

COMMUNICATION

Mononuclear Nonheme Iron(IV)-Oxo and Manganese(IV)-Oxo Complexes in Oxidation Reactions: Experimental Results Prove Theoretical Prediction†

Received 00th January 20xx,
Accepted 00th January 20xx

DOI: 10.1039/x0xx00000x

www.rsc.org/

Junying Chen,‡ Kyung-Bin Cho,‡ Yong-Min Lee, Yoon Hye Kwon, and Wonwoo Nam*

Reactivities of mononuclear nonheme iron(IV)-oxo and manganese(IV)-oxo complexes bearing a pentadentate N4Py ligand, $[M^{IV}O(N4Py)]^{2+}$ (M = Fe and Mn), are compared in hydrogen atom transfer (HAT) and oxygen atom transfer (OAT) reactions; theoretical and experimental results show that $Fe^{IV}O$ is more reactive than $Mn^{IV}O$. The latter is shown to react through excited state reactivity (ESR).

High-valent metal-oxo intermediates have been invoked as key intermediates in biological and chemical oxidation reactions.[1-3] Recently, mononuclear nonheme $Fe^{IV}O$ complexes have been well studied in a variety of oxidation reactions;[3] factors that affect the reactivities of the $Fe^{IV}O$ complexes have been extensively studied, such as the structure and topology of supporting ligands, the spin state of metal ions, and the cooperation of Lewis acid and axial ligand.[3-6] In contrast to the well-studied nonheme $Fe^{IV}O$ complexes, there are only a few number of mononuclear nonheme $Mn^{IV}O$ complexes synthesized in biomimetic systems,[7-11] although Mn-oxo species are known to play a decisive role in enzymatic and catalytic oxidation reactions, such as in oxygen-evolving complex (OEC) in Photosystem II.[12] Recently, we have shown that mononuclear nonheme $Mn^{IV}O$ complexes are capable of oxidizing the C−H bonds of alkanes as strong as cyclohexane[9] and that the oxidizing power of the $Mn^{IV}O$ complexes could be enhanced even beyond that of $Fe^{IV}O$ oxidants by binding redox-inactive metal ions or triflic acid.[10,11]

From a theoretical perspective, $Mn^{IV}O$ was shown to perform hydrogen atom transfer (HAT) reactions by using an excited state configuration,[13] referred below as excited state reactivity (ESR) for convenience. In ESR, the electron in the π^*_{xz} orbital of the $Mn^{IV}O$ moiety is excited into the σ^*_{xy} orbital, and the substrate is subsequently interacting with the empty π^*_{xz} orbital. This ESR is higher in energy at the reactant state, but may have lower transition state (TS) than the other alternatives and avoids potentially inefficient spin flips.[13] For instance, to use the otherwise low energy barrier of S = 1/2 state, spin flips are required both before and after the reaction to produce the S = 2 $Mn^{III}OH$ product, raising questions about its efficiency. A more detailed description of ESR is found in the previous publication.[13]

In the case of $Fe^{IV}O$, most synthetic species are known to have S = 1 spin state as reactants, but both S = 1/2 and S = 5/2 are possible at the $Fe^{III}OH$ stage, depending on the external conditions.[14] Hence, a spin state may or may not occur. As the energy barriers are usually lowest in the S = 2 state due to exchange enhanced reactivity,[2] this reaction has been mostly assumed to be perfomed in the S = 2 state through two state reactivity (TSR), but this would ultimately depend on the spin inversion probability.[15]

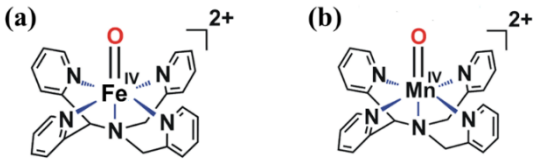

Fig. 1 Schematic drawing of the chemical structures of (a) $[Fe^{IV}O(N4Py)]^{2+}$ (**1**) and (b) $[Mn^{IV}O(N4Py)]^{2+}$ (**2**), N4Py = *N*,*N*-bis(2-pyridylmethyl)-*N*-bis(2-pyridyl)methylamine.

Comparisons between $Fe^{IV}O$ and $Mn^{IV}O$ therefore contains many interesting questions, such as the reactivity of the both species, and consequently the efficiency of ESR *versus* TSR. Indeed, comparisons between these two species are seen scattered throughout the previous studies. For instance, Georgiev *et al*. have compared two dioxygenase reactions theoretically each containing an Fe and Mn active centre, respectively.[16] They found that the reaction mechanisms are similar, albeit with different rate-determining steps (r.d.s.). Barman *et al*. reported the influence of ligand structures on oxidation reactions by

Department of Chemistry and Nano Science, Ewha Womans University, Seoul 120-750 (Korea). Fax: (+82)-2-3277-4114; E-mail: wwnam@ewha.ac.kr
† Electronic Supplementary Information (ESI) available: Experimental details of kinetics, theoretical procedures and methods, energies, selected Mulliken spin density distributions and geometries. See DOI: 10.1039/x0xx00000x
‡ These authors contributed equally to this study.

$Mn^{IV}O$ species with two isomers of a bispidine ligand which showed an inversed order of reactivities compared with that of $Fe^{IV}O$.[7] In addition, we have published earlier the reactivities of $Fe^{IV}O$ and $Mn^{IV}O$ species bearing N4Py or Bn-TPEN ligands, although the reactivity studies were done separately and under different experimental conditions.[4,6,9-11,13-15] Herein, we report a theoretical comparison of the reactivities of high-valent metal-oxo species, $[Fe^{IV}O(N4Py)]^{2+}$ (**1**) and $[Mn^{IV}O(N4Py)]^{2+}$ (**2**) (Fig. 1), towards HAT and oxygen atom transfer (OAT) reactions under *identical settings*. This is followed by experimental results obtained by carrying out the reactions under *identical conditions*. The results provide evidence that $Fe^{IV}O$ (**1**) is more reactive than $Mn^{IV}O$ (**2**) in the HAT and OAT reactions.

The DFT energy barrier for the HAT reaction with **1** and 1,4-cyclohexadiene (CHD) is calculated to be 13.4 and 12.3 kcal mol^{-1} for S = 1 and 2, respectively. We have earlier estimated the spin inversion of **1** to correspond to 3.4 kcal mol^{-1} in additional barrier, if using cyclohexene.[15] The use of CHD in our present study has the potential of modifying this value somewhat, but the correction should still be minor compared to the targeted error margins of DFT (±3 kcal mol^{-1}). Hence, we add this value to the barrier as is, if making a spin state transition. We would therefore theoretically expect an S = 2 barrier of about 12.3 + 3.4 = 15.7 kcal mol^{-1}. This would make the S = 2 barrier larger than the S = 1 barrier, hence it becomes unfavourable. Complicating the matters is that there probably are some tunnelling in this reaction,[17] but its magnitude is not expected to change our conclusions as we have shown before in the $Fe^{IV}O$ case that its effects do not exceed 2 kcal mol^{-1}.[15] Therefore, from the current data, the reaction is predicted to occur at the S = 1 surface over a barrier of about 13.4 kcal mol^{-1}, but the S = 2 reaction cannot be excluded as the barrier height and overall reaction energy differences are small.

In the reaction with **2**, a low S = 1/2 barrier of 16.2 kcal mol^{-1} was found (Fig. 2, black), which is in line with other $Mn^{IV}O$ studies.[7,13] For the S = 3/2 state, no less than three reaction pathways were found. The first alternative transfers an α-electron to the $\sigma^*_{z^2}$ orbital during the HAT (Fig. 2, red), utilizing the so called σ-channel, confirmed by an Mn-O-H angle of 170° at the TS (Table S20, ESI†). This electron relaxes down to the σ^*_{xy} orbital at the intermediate stage. Direct electron transfer to σ^*_{xy} from the substrate is not possible as this orbital lacks spin density on O. The second alternative transfers a β-electron to the π^*_{xz} orbital, which subsequently relaxes down to δ (Fig. 2, green). The third pathway utilizes ESR by first exciting the π^*_{xz} electron to σ^*_{xy} (Fig. 2, grey). In our previous work with cyclohexane as substrate, the presence of substrate stabilized this excited state and allowed us to locate this species 15.5 kcal mol^{-1} higher in energy than the ground state.[13] In the present case with a weak C-H bond (78 kcal mol^{-1})[18] CHD as substrate, no stabilization of this excited state was found. Instead, the reactant either reverted to its ground state configuration, or it broke the weak C-H bond to abstract a proton and an α-electron to π^*_{xz} (Fig. 2, blue). However, albeit not stable, it was clear that there was an energy plateau about 15.3 kcal mol^{-1} up in energy which corresponded to this excited state (see ESI,† DFT section - Free Energy Calculations). As this value is lower than the S = 1/2 barrier of 16.2 kcal mol^{-1} and two spin inversions are avoided, we propose that this transition to the excited state of 15.3 kcal mol^{-1} is the *de facto* energy barrier, which will optimize directly to the $Mn^{III}O^{\bullet}$ structure. Despite this interesting feature of **2**, it is however clear that the reactivity of **1** is predicted to be one or two order of magnitudes larger than **2** in terms of rates.

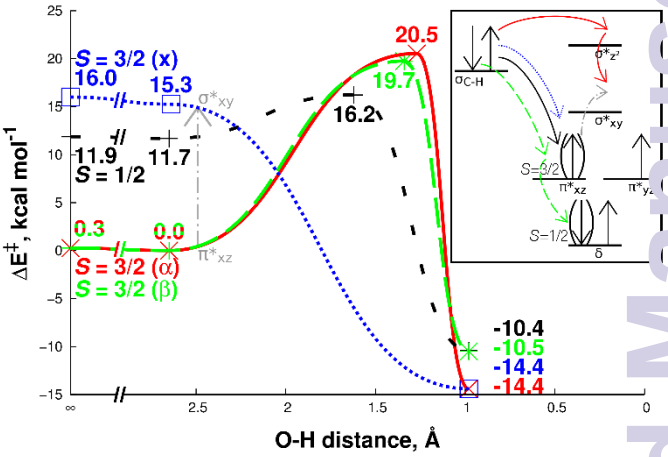

Fig. 2 Reaction energy profile for the HAT reaction by **2** in the S = 1/2 state (black, short dashes, +), S = 3/2 α-electron transfer (red, solid, X), S = 3/2 β-electron transfer (green, long dashes, ✳), and the S = 3/2 excited state (x) reaction (blue, dots, □). The x-axis is projected along the shrinking O-H bond length. The energy values are indicated at a stationary point. The inset shows the electron occupation at either S = 1/2 ($\delta^2,\pi^*_{xz}{}^0,\pi^*_{yz}{}^2$) or S = 3/2 ($\delta^1,\pi^*_{xz}{}^1,\pi^*_{yz}{}^1$) state and the subsequent electron transfer during the HAT reaction in the different states (see the text for details). The lowest energy pathway is proposed to be an α-electron excitation from π^*_{xz} to σ^*_{xy} (grey, dash-dot) in the S = 3/2 state, whereby the reaction relaxes directly to the intermediate $Fe^{III}OH$ structure.

In experiments, **1** and **2** were generated by reacting the corresponding M^{II}(N4Py) complexes with iodosylbenzene (PhIO) in a solvent mixture of CF_3CH_2OH-CH_3CN (*v/v* = 19:1) at 298 K, as reported previously (Fig. S1a, ESI†).[4,10] Subsequent studies on the HAT reactivities with substrates having BDEs[18] between 77 kcal mol^{-1} (9,10-dihydroanthracene) and 90 kcal mol^{-1} (toluene) by **1** and **2** were carried out. Addition of these substrates to the solutions of **1** and **2** at 298 K resulted in the disappearance of the absorption bands at 695 nm for **1** and 940 nm for **2**, respectively (Fig. S1b and S1c, ESI†). The first-order rate constants (k_{obs}), determined by pseudo-first-order fitting of the kinetic data for the decay at 695 nm due to **1** and at 940 nm due to **2**, increased proportionally with the increase of substrate concentration, whereby second-order rate constants (k_2) were determined (see Table S1 and Fig. S2 and S3, ESI†). In the case of CHD, the second-order rate constants for **1** and **2** were 64(5) and 6.2(4) M^{-1} s^{-1}, indicating that **1** is, by a factor of 10, more reactive than **2** (Fig. 3a). The same trends were obtained with other substrates, and Fig. 3b shows a good linear correlation between log k_2' and the C-H BDEs of the substrates. In addition, a kinetic isotope effect (KIE) value of 44 and 11 were obtained in the oxidation reactions of cumene-h_{12} and -d_{12} by **1** and **2**, respectively (Fig. S4, ESI†). The large KIE value and the good correlation between log k_2' and the substrate BDEs clearly indicate that the C-H bond activation of alkanes by **1** and **2** occurs *via* a HAT which is the r.d.s. Using the Eyring equation, the experimentally obtained k_2' values for CHD above

correspond to 16.2 and 17.2 kcal mol^{-1} in energy barrier at 298 K. This is to be compared to our "best" DFT calculated values of 13.4 and 15.3 kcal mol^{-1}, in agreement with experiments that **1** is a better oxidant showing higher reactivity than **2**.

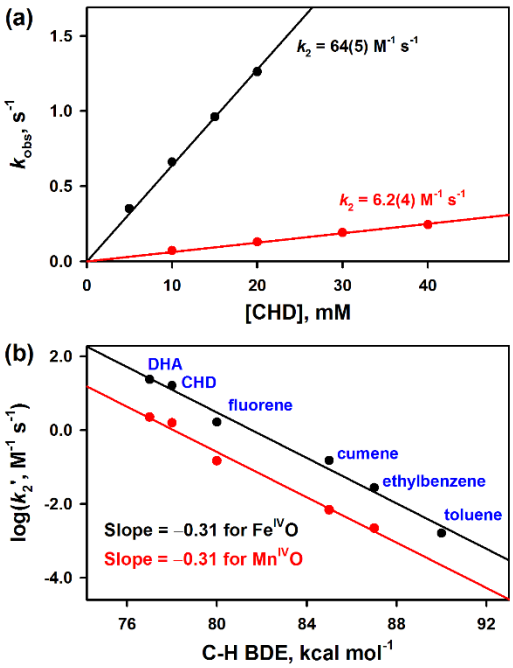

Fig. 3 Oxidation reactions by **1** (black circles) and **2** (red circles) in CF_3CH_2OH:CH_3CN (*v*/*v* = 19:1) at 298 K. (a) Plots of the pseudo-first-order rate constants (k_{obs}) against the concentration of CHD to determine k_2 in the oxidation reaction of CHD. (b) Plots of log k_2' against the C–H BDEs of various hydrocarbons. k_2' were obtained by dividing k_2 by the number of equivalent target C-H bonds in the substrates.

Turning our attention to sulfoxidation reactions, a deeper insight can be gained by investigating the participating orbitals in this reaction. Upon M-O bond elongation, the π_{xz} and π^*_{xz} orbitals break up into their localized constituent orbitals, d_{xz} on M and p_x on O. The π_{yz}/π^*_{yz} and $\sigma_{z^2}/\sigma^*_{z^2}$ pairs undergo similar decomposition, forming d_{yz} and d_{z^2} orbitals on M and p_y and p_z on O, respectively. Meanwhile, if the reaction occurs through the so-called π-channel, p_x starts to form the bonding (and anti-bonding) σ-orbitals with the hybrid sp^2 lone pair orbital of S. The M-O-S angle in this case would ideally be 90° due to the orbital overlap between p_x and sp^2. Due to steric constraints, this angle is around 130° with the N4Py ligand. However, if the reaction occurs through the σ-channel, the p_z orbital is interacting with sp^2 instead, resulting in an ideal attacking angle of 180°. We detail in ESI† a more in-depth discussion about the interacting orbitals and electron transfers (Fig. S5, ESI†).

The DFT calculated barrier for thioanisole reaction with **1** is 19.7 and 10.5 kcal mol^{-1} for S = 1 and 2, respectively. Given that the product Fe^{II} is an S = 2 species, while **1** is S = 1, it is clear that a spin transition has to occur during the reaction. Hence, if making a spin state transition before the TS, we would therefore theoretically expect an S = 2 barrier of about 10.5 + 3.4 = 13.9 kcal mol^{-1}, adding the energy required for spin inversion. This barrier would still be smaller than the S = 1 barrier. In addition, we found that sulfoxidation in the S = 1 state utilizes ESR as well (see ESI† DFT section for details). Due to the much lower S = 2 energy barrier, we suggest that this reaction occurs through the S = 2 TS, which utilizes the σ-channel.

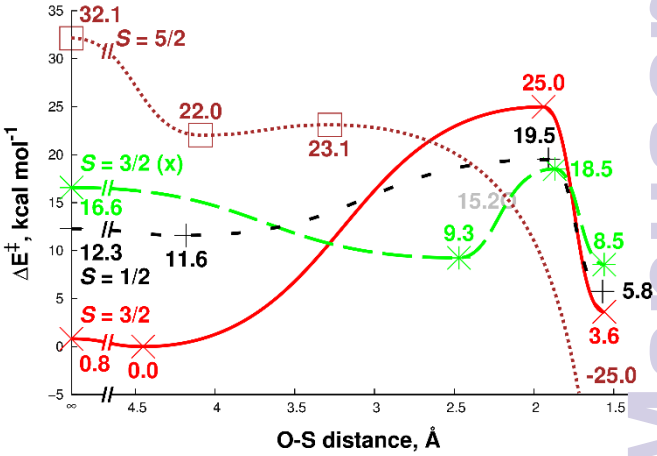

Fig. 4 Reaction energy profile for thioanisole sulfoxidation by **2**. The x-axis is along the shrinking O-S distance of this reaction. The interacting orbitals in π- and σ-channel reactions are also shown (see text and ESI†). The excited S = 3/2 state (green, mark… "(x)") has the lowest TS at 18.5 kcal mol^{-1}, but the MECP (15.2 kcal mol^{-1}, marked in gre… may act as a lower TS, depending on the spin inversion probability.

For **2**, the calculations show a multitude of possible pathways. Here, while the reactant **2** is in the S = 3/2 state, the product Mn^{II} is an S = 5/2 species. Hence, a spin state change ha… to occur along the reaction. While the bare S = 5/2 state of **2** … unattainable due to its high energy (32.1 kcal mol^{-1}; Fig. 4, brown), it immediately abstracts an electron from the substra… upon complexation to form Mn^{III}O and a substrate radical, whic… lowers the system energy by 10.1 kcal mol^{-1}. However, this … still too high to be relevant at this stage of the reaction. Instead, the S = 3/2 excited state ("x"; Fig. 4, green) was found to b… stable upon complexation. The reason for this stability is that a partial electron transfer occurs upon complexation, lowering … system energy by 7.3 kcal mol^{-1} to become 9.3 kcal mol^{-1} above the ground state. This is seen through Mulliken spin density distribution (ESI†, Table S14), where the substrate ha… developed a β-spin of 0.4. The TS for this spin state is at 18… kcal mol^{-1}, which is energetically lowest of them all and feature… a π-channel interaction. A spin state change is then required … the end of the reaction to reach S = 5/2. Alternatively, the spi… state change could occur before the TS, at the minimum energ… crossing point (MECP) which was found to be at 15.2 kcal mol^{-1} (Fig. 4, grey). This value would then be the r.d.s. Indeed, r.d… spin crossing TS has been postulated before in a Mn-containing dioxygenase system.[16] As this value is likely to be adjusted up somewhat due to spin inversion probability, the r.d.s. bar… value is best given as a range value between 15.2 and 18.5 kca… mol^{-1}. The normal S = 3/2 ground state is deemed to have to… high TS (25 kcal mol^{-1}) to be feasible (Fig. 4, red) and the S … 1/2 state would require an initial spin flip before the reaction, followed by two β-electron flips after the reaction to obtain an S = 5/2 product, which was deemed unlikely. The overall conclusion, however, is that **1** has a lower barrier than **2** … sulfoxidation reactions as well.

The reactivity of **1** in OAT reactions was investigated experimentally in CF_3CH_2OH:CH_3CN (*v*/*v* = 19:1) at 273 K, as the reactivity of **2** in OAT reactions was reported previously.[10] Addition of *para*-X-thioanisoles (X = OMe, Me, H, F, and Br) to the solution of **1** resulted in the disappearance of the absorption bands at 695 nm due to **1** (Fig. S6, ESI†). The first-order rate constants (k_{obs}) increased linearly with increasing substrate concentration, leading us to determine a second-order rate constant (k_2; see Table S2 and Fig. S7, ESI†). In the oxidation reactions of thioanisole by **1** and **2**, **1** (k_2 = 1.1(1) M^{-1} s^{-1}) is ~120 times more reactive than **2** (k_2 = 9.2(7) × 10^{-3} M^{-1} s^{-1}).[10] Further, as shown in Fig. 5, when log k_2 were plotted against the oxidation potential (E_{ox}) of thioanisole derivatives, a good linear correlation with slopes of –6.2 for **1** and –8.2 for **2** was obtained (see also Fig. S8 for Hammett plots). The experimental k_2 values should correspond to 15.8 and 18.5 kcal mol^{-1} in energy barrier at 273 K for **1** and **2**, respectively, to be compared to the theoretical values obtained above (13.9 *vs.* 15.2 kcal mol^{-1}).

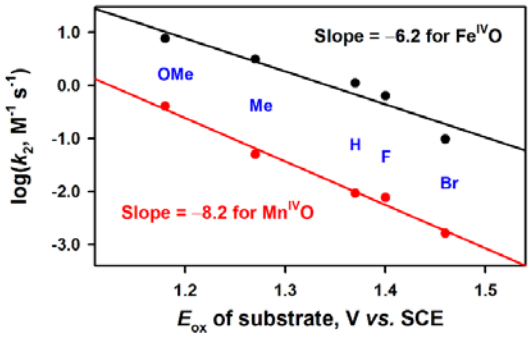

Fig. 5 Plots of log k_2 against one-electron oxidation potentials (E_{ox}) of *para*-X-thioanisole derivatives (X = MeO, Me, H, F, and Br) for **1** (black circles) and **2** (red circles)[10] in CF_3CH_2OH-CH_3CN (*v*/*v* = 19:1) at 273 K (see Table S2).

In summary, we have conducted a combined theoretical and experimental study for the reactivity comparisons of $Fe^{IV}O$ and $Mn^{IV}O$ complexes in HAT and OAT reactions. Both theory and experiments agree that under the investigated conditions with the N4Py ligand, $Fe^{IV}O$ is a stronger oxidant than its $Mn^{IV}O$ counterpart. In addition, $Mn^{IV}O$ is again confirmed to be likely to react through ESR rather than TSR, as found earlier.[13]

This work was supported by the NRF of Korea through CRI (NRF-2012R1A3A2048842 to W.N.), GRL (NRF-2010-00353 to W.N.) and MSIP (2013R1A1A2062737 to K.-B.C.).

Notes and references

1 (a) M. M. Abu-Omar, A. Loaiza and N. Hontzeas, *Chem. Rev.*, 2005, **105**, 2227; (b) I. G. Denisov, T. M. Makris, S. G. Sligar and I. Schlichting, *Chem. Rev.*, 2005, **105**, 2253; (c) J. T. Groves, *J. Inorg. Biochem.*, 2006, **100**, 434; (d) P. R. Ortiz de Montellano, *Chem. Rev.*, 2010, **110**, 932; (e) S. Shaik, S. Cohen, Y. Wang, H. Chen, D. Kumar and W. Thiel, *Chem. Rev.*, 2010, **110**, 949; (f) C. Krebs, D. G. Fujimori, C. T. Walsh and J. M. Bollinger, Jr, *Acc. Chem. Res.*, 2007, **40**, 484; (g) W. Nam, *Acc. Chem. Res.*, 2007, **40**, 522; (h) P. C. A. Bruijnincx, G. van Koten and R. J. M. Klein Gebbink, *Chem. Soc. Rev.*, 2008, **37**, 2716; (i) A. S. Borovik, *Chem. Soc. Rev.*, 2011, **40**, 1870; (j) J. Hohenberger, K. Ray and K. Meyer, *Nat. Commun.*, 2012, **3**, 720; (k) K. Ray, F. F. Pfaff, B. Wang and W. Nam, *J. Am. Chem. Soc.*, 2014, **136**, 13942; (l) K. Ray, F. Heims, M. Schwalbe and W. Nam, *Curr. Opin. Chem. Biol.*, 2015, **25**, 159; (m) P. Comba, M. Kerscher and W. Schiek, *Prog. Inorg. Chem.*, 2007, **55**, 613; (n) A. Bakac, *Coord. Chem. Rev.*, 2006, **250**, 2046; (o) J. H. Espenson, *Coord. Chem. Rev.*, 2005, **249**, 329; (p) H. Fujii, *Coord. Chem. Rev.*, 2002, **226**, 51; (q) E. I. Solomon, T. C. Brunold, M. I. Davis, J. N. Kemsley, S.-K. Lee, N. Lehnert, F. Neese, A. J. Skulan, Y.-S. Yang and J. Zhou, *Chem. Rev.*, 2000, **100**, 235; (r) M. Costas, M. P. Mehn, M. P. Jensen and L. Que, Jr, *Chem. Rev.*, 2004, **104**, 939; (s) E. I. Solomon, S. D. Wong, L. V. Liu, A. Decker and M. S. Chow, *Curr. Opin. Chem. Biol.*, 2009, **13**, 99; (t) K.-B. Cho, E. J. Kim, M. S. Seo, S. Shaik and W. Nam, *Chem. Eur. J.*, 2012, **18**, 10444.

2 D. Usharani, D. Janardanan, C. Li and S. Shaik, *Acc. Chem. Res.*, 2013, **46**, 471.

3 W. Nam, Y.-M. Lee and S. Fukuzumi, *Acc. Chem. Res.*, 2014, **47**, 1146.

4 J. Kaizer, E. J. Klinker, N. Y. Oh, J.-U. Rohde, W. J. Song, A. Stubna, J. Kim, E. Münck, W. Nam and L. Que, Jr, *J. Am. Chem. Soc.*, 2004, **126**, 472.

5 (a) S. Hong, Y.-M. Lee, K.-B. Cho, K. Sundaravel, J. Cho, M. J. Kim, W. Shin and W. Nam, *J. Am. Chem. Soc.*, 2011, **133**, 11876; (b) P. Leeladee, R. A. Baglia, K. A. Prokop, R. Latifi, S. P. de Visser and D. P. Goldberg, *J. Am. Chem. Soc.*, 2012, **134**, 10397; c) S. Sahu, M. G. Quesne, C. G. Davies, M. Dürr, I. Ivanović-Burmazović, M. Siegler, G. N. L. Jameson, S. P. de Visser and D. P. Goldberg, *J. Am. Chem. Soc.* 2014, **136**, 13542. d) S. Sahu, L. R. Widger, M. G. Quesne, S. P. de Visser, H. Matsumura, P. Moënne-Loccoz, M. A. Siegler and D. P. Goldberg, *J. Am. Chem. Soc.* 2013, **135**, 10590.

6 J. Park, Y.-M. Lee, W. Nam and S. Fukuzumi, *J. Am. Chem. Soc.*, 2013, **135**, 5052.

7 P. Barman, A. K. Vardhaman, B. Martin, S. J. Wörner, C. V. Sastri and P. Comba, *Angew. Chem., Int. Ed.*, 2015, **54**, 2095.

8 (a) G. Yin, *Acc. Chem. Res.*, 2013, **46**, 483; (b) S. Shi, Y. Wang, A. Xu, H. Wang, D. Zhu, S. B. Roy, T. A. Jackson, D. H. Busch and G. Yin, *Angew. Chem., Int. Ed.*, 2011, **50**, 7321; (c) Y. Wang, S. Shi, H. Wang, D. Zhu and G. Yin, *Chem. Commun.*, 2012, **48**, 7832; (d) S. G. Sawant, X. Wu, J. Cho, K.-B. Cho, S. H. Kim, M. S. Seo, Y.-M. Lee, M. Kubo, T. Ogura, S. Shaik and W. Nam, *Angew. Chem., Int. Ed.* 2010, **49**, 8190; (e) D. F. Leto, R. Ingram, V. W. Day and T. A. Jackson, *Chem. Commun.*, 2013, **49**, 5378.

9 X. Wu, M. S. Seo, K. M. Davis, Y.-M. Lee, J. Chen, K.-B. Cho, Y. N. Pushkar and W. Nam, *J. Am. Chem. Soc.*, 2011, **133**, 20088.

10 J. Chen, Y.-M. Lee, K. M. Davis, X. Wu, M. S. Seo, K.-B. Cho, H. Yoon, Y. J. Park, S. Fukuzumi, Y. N. Pushkar and W. Nam, *J. Am. Chem. Soc.*, 2013, **135**, 6388.

11 (a) H. Yoon, Y.-M. Lee, X. Wu, K.-B. Cho, R. Sarangi, W. Nam and S. Fukuzumi, *J. Am. Chem. Soc.*, 2013, **135**, 9186; (b) J. Chen, H. Yoon, Y.-M. Lee, M. S. Seo, R. Sarangi, S. Fukuzumi and W. Nam, *Chem. Sci.*, 2015, **6**, 3624.

12 (a) J. Yano, J. Kern, K. Sauer, M. J. Latimer, Y. Pushkar, J. Biesiadka, B. Loll, W. Saenger, J. Messinger, A. Zouni and V. K. Yachandra, *Science*, 2006, **314**, 821; (b) A. Guskov, J. Kern, A. Gabdulkhakov, M. Broser, A. Zouni and W. Saenger, *Nat. Struct. Mol. Biol.*, 2009, **16**, 334; (c) P. E. M. Siegbahn, *J. Am. Chem. Soc.*, 2009, **131**, 18238; (d) P. E. M. Siegbahn and R. H. Crabtree, *J. Am. Chem. Soc.*, 1999, **121**, 117.

13 K.-B. Cho, S. Shaik and W. Nam, *J. Phys. Chem. Lett.*, 2012, **3**, 2851.

14 K.-B. Cho, X. Wu, Y.-M. Lee, Y. H. Kwon, S. Shaik and W. Nam, *J. Am. Chem. Soc.*, 2012, **134**, 20222.

15 Y. H. Kwon, B. K. Mai, Y.-M. Lee, S. N. Dhuri, D. Mandal, K.-B. Cho, Y. Kim, S. Shaik and W. Nam, *J. Phys. Chem. Lett.*, 2015, **6**, 1472.

16 V. Georgiev, T. Borowski, M. R. A. Blomberg and P. E. M. Siegbahn, *J. Biol. Inorg. Chem.*, 2008, **13**, 929.

17 D. Mandal, R. Ramanan, D. Usharani, D. Janardanan, B. Wang and S. Shaik, *J. Am. Chem. Soc.*, 2015, **137**, 722.

18 Y.-R. Luo, *Handbook of Bond Dissociation Energies in Organic Compounds*, CRC Press, New York, 2003.

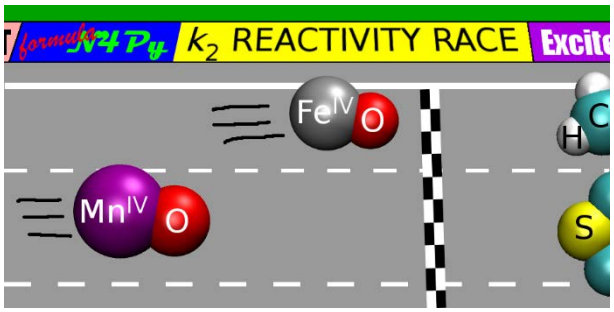

Graphical abstract. The HAT and OAT reactivities of $Fe^{IV}O$ and $Mn^{IV}O$ species with N4Py ligand are compared both theoretically and experimentally and shown to be faster for $Fe^{IV}O$.